AN APPLICATION ANALYSIS APPROACH FOR NOISE ESTIMATION IN PANORAMIC X-RAY IMAGES

Peter Michael Goebel, Ahmed Nabil Belbachir
Vienna University of Technology
Pattern Recognition and Image Procesing Group
Favoritenstraße 9/183-2, A-1040 Vienna, Austria.
goe,nabil@prip.tuwien.ac.at

Abstract:
This paper presents an appropriate approach for the estimation of noise statistics in dental panoramic X-ray images on a system (Orthophos/DÜRR) with a storage phosphor plate as sensor. Many state of the art methods use multi scale filtering of images to reduce the irrelevant part of information, based on generic estimation of noise. The usual assumption of a distribution of Gaussian and Poisson statistics only leads frequently to overestimation of the noise variance in regions of low intensity (small photon counts), but to underestimation in regions of high intensity and therefore to non-optimal results after denoising the image.
In this paper, an analysis of the real noise statistics in the case of dental panoramic X-ray images is performed. The goal is to form a tractable model of the noise statistics to achieve maximum image quality after denoising. The analysis approach is tested on 2000 samples from a database of 50 panoramic X-ray images and the results are cross validated by medical experts.

1 Introduction

In medical diagnostics intuitive decisions take place, based on experience, besides the medical knowledge. Therefore, preservation of the overall look of an image, even though after application of an image processing method, is prominent. Appropriate methods have often to deal with detection of small, low contrast image details, situated side by side, differing probably not in gray-level-mean, but may have slightly different variance. According to Weber's law [18], the *Just Noticeable Difference* (JND), which is *"'the differential threshold to produce a noticeable variation in a sensory input that is perceivable by a human being or other animal"'*, has to be preserved. Among others, most used methods for image denoising are multiscale

filtering based on the wavelet transform [14, 16]. The basic idea is to decompose an image into different contributions in several frequency bands and at different scales, leading to a (over complete) representation in the transformed space. Thus, the deterministic image content is represented by a set of few stronger coefficients, whereas the noise is spread over all coefficients with weakly strength. Therefore, a deconvolution technique is usually applied using linear or non-linear filtering [4, 14] to reduce the contribution of noise in the transformed coefficients. Denoising by thresholding the wavelet coefficients [4], using a threshold, derived from an overestimated noise variance estimate, easily remove weakly details, whereas doing so with an underestimated ones, keeps the noise in areas of constant contrast. The works in [2, 3] evaluate the efficiency of denoising and enhancement using simulations of X-ray images contaminated by additive noise of known distribution. Most approaches suppose the noise has Gaussian nature; some suppose a Poisson distribution or a mixture of both distributions.
However, X-ray images show neither the Gaussian nor the Poisson distribution alone. The noise is coherent to the density of matter, because of effects of scattering, consequently the noise variance is spatially adaptive, too. Therefore, an accurate investigation on the noise model has to be performed for optimal denoising results.
Some attempts of authors to preserve the edges within an image fail in the case of low contrasts. The estimation of noise itself is left open by many authors. A comparative study between six methods is shown in [9]. A method for blind estimation of noise variance is given in [6] and the references therein. Statistical models for images are descibed in [11] and the references therein.

1.1 Panoramic Radiography

A technique, where the entire dentition is projected onto a sensing device is termed Dental Panoramic Radiography (DPR). Source and detector are in opposition, rotated around the patients head. The focal area of the X-ray beam describes a planar curve, which is standardized for the human teeth and jaws. An irradiation model, consisting of three parts, X-ray source, interaction of the beam with matter and imaging of the remaining photons build up for the physics of such a radiographic process. The X-ray source is operated at a certain *kilo-Voltage-peak* (kVp), which, along with any filtration, determines the energy spectrum of the beam [1, 10].

1.2 Scattering of Photons

As an X-ray beam travels trough matter, individual photons are removed, the beam intensity is stochastically predictable (see Figure- 1). Three processes are significant for projection radiography: Photoelectric, Coherent and Compton scatter absorption.

Photoelectric absorption occurs when an incident photon collides with an inner-shell electron,

in an atom of the absorbing medium, resulting in total absorption and the incident photon ceases to exist. The electron is ejected from its shell, resulting in ionization and becomes a recoil electron (photo electron). The kinetic energy imparted to the recoil electron is equal to the energy of the incident photon minus that used to overcome the binding energy of the electron. Roughly speaking, suppose 100 kVp, up to 30% of photons from an X-ray beam, are absorbed by the photoelectric process.

Coherent Scattering (Thomson scattering) may occur when a low-energy incident photon passes near an outer electron of an atom, which has low binding energy. The incident photon interacts with the electron, in the outer-shell, by causing it to vibrate momentarily at the same frequency as the incoming photon. The incident photon then ceases to exist. The vibration causes the electron to radiate energy in the form of another x-ray photon with the same frequency and energy as in the incident photon. In effect, the direction of the incident x-ray photon is altered. Coherent scattering contributes very little to noise fog because the total quantity of scattered photons is small (around 8%) and its energy level is too low for much of it to reach the sensor.

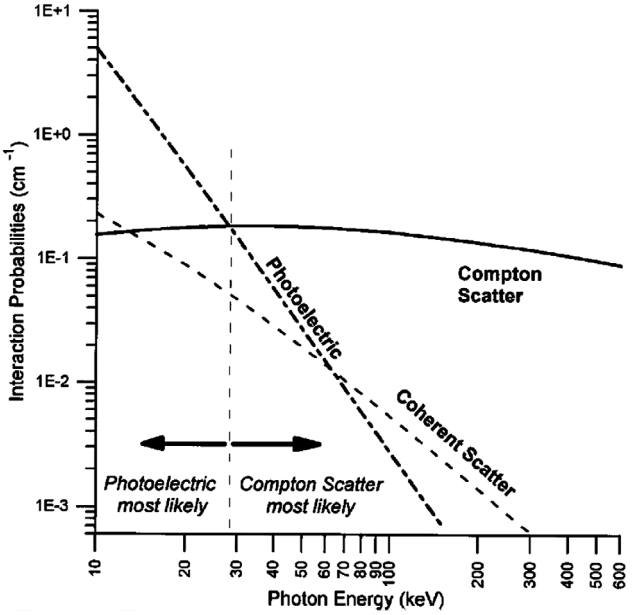

Figure 1: Relationship of Interaction Probabilities for Coherent-, Photoelectric- and Compton Scatter to Photon Energy [13].

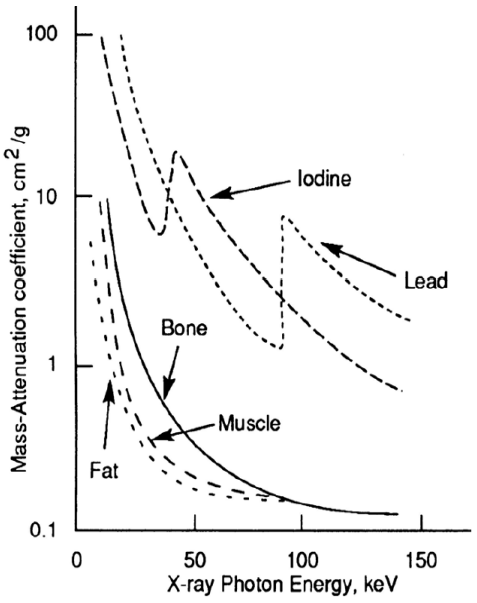

Figure 2: Non-linear Relationship between Photon Energy and Mass Attenuation for Various Tissue [10].

Compton scattering (Incoherent scattering) occurs when a photon interacts with an outer electron, which is then deflected by its interaction and is scattered. The energy of the scattered photon equals the energy of the incident photon minus the kinetic energy gained by the recoil electron plus its bonding energy. As with photoelectric absorption, Compton scattering results in the loss of an electron and ionization of the absorbing atom. Thus, the probability of Compton scattering is directly proportional to the electron density. The number of

electrons in bone is greater than in water, therefore the probability of Compton scattering is correspondingly greater in bone than in tissue. In a dental x-ray beam, approximately up to 62% of the photons undergo Compton scattering.

1.3 Mass-Energy Attenuation

X-ray photons from the source, which have Poisson statistics, are absorbed along the path between the source and detector by the patient's matter (muscle, fat, bone, air, or contrast agents). The photon attenuation of each type of matter depends on its elementary and chemical composition as well as the beam. This effect is quantified by the linear mass attenuation coefficient μ, in units cm^2/g, which gives the fraction of photons that are absorbed by unit thickness of matter [5]. Unfortunately, μ is not a constant and varies by Photoelectric absorption, coherent scatter and Compton scatter [1, 10]. Figure- 2 shows the non-linear relationship between photon energy and mass attenuation for bone, fat and muscle [10].
Quantitatively, the attenuation by absorption is given by μdz for an infinitesimal sheet of thickness dz at depth z from the exterior of matter, facing the X-ray source. Thus, the intensity $I(z)$ is the solution of the differential equation $\frac{dI}{I(z)} = -\mu dz$, with initial condition $I_0 = I(z = 0)$, the intensity at z=0, gives:

$$I(z) = I_0 \ \exp(-\mu z) = I_0 \ \exp(-\frac{\alpha}{\rho} \ (\rho x)) \tag{1}$$

where α is the linear attenuation coefficient in units of cm^{-1}, density ρ in units g/cm^3, x in cm and z has units g/cm^2. Other names are coefficient of linear absorption, coefficient of linear attenuation or the macroscopic cross-section. The total cross-section of a substance is the sum of all partial cross-sections, which are also a function of energy of the incident photons. The attenuation process goes proportional to the incident energy E into Photo-ionization with E^{-3} and Atomic-number Z^4, whereas for Compton scattering more than $> E^{-3}$ and proportional to Z. Figure- 1 shows the probabilities of scatter type depending on photon energy. However, the energy spectrum of an X-ray tube is not monochromatic, but the beam is hardened due to absorption of low energy photons by matter. Thus, an aluminum or other filter is mandatory to absorb low energy photons, to prevent unnecessarily increasing the patients dose.

2 The Problem Statement

The goal is to find better estimates for the noise variance in panoramic X-ray images. The motivation comes from the experience, that the simplifying assumption of *Independently Identically Distributed* (IID) noise statistics may lead to an error in estimation of the noise variances. Thus, in real X-ray images one can find a significant coherence of the noise with the

image contents. Furthermore, if one assumes Poisson statistics only, the results are often unsatisfactory.

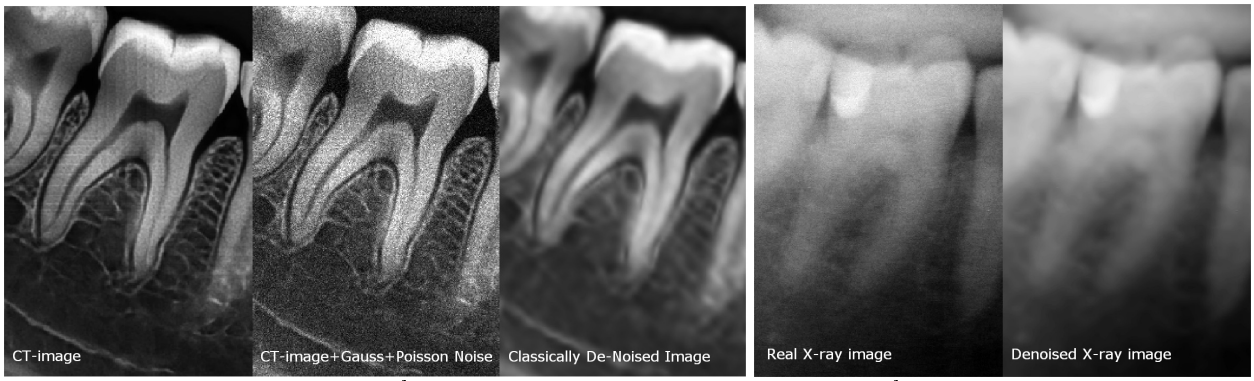

Figure 3: CT image as a reference a); Gaussian and Poisson Noise added b); denoised by classical soft-thresholding c); Real X-ray Image d); and the denoised variant e).

To illustrate the problem, two panoramic image acquisitions are depicted: Figure 3 a) shows an image from *Computer Tomography* scan technique (CT) and another image Figure 3 d) from *Computer Radiography* (CR) X-ray imaging. One can say, the CT image in Figure 3 a) shows an idealistic view of the real panoramic X-ray image. Figure 3 b) shows the degradation of the image quality if a mixture of Gaussian and Poisson noise is added to the CT image, where the resulting image quality is still far from that of Figure 3 d). A classical denoising approach is performed by wavelet coefficients soft-thresholding using an usually noise estimate [4]. Figure 3 c) shows the noise mainly removed, but the image is blurred. Within the weak wavelet coefficients there is hidden edge information, therefore fine details in the image are lost (pseudo-Gibbs phenomenon). Figure 3 e) shows the effect of such a denoising on the real image. It seems, the low contrast image is more sensitive than the CT image to the overestimated noise estimate.
Therefore, a model for estimation of noise is constructed, which operates blind, thus a second signal estimate provides the required information.

3 X-ray Photon Propagation Model

The X-ray generator in Fig. 4 produces photons with Poisson count statistic; the arrival-time difference between successive Poisson counts is Gamma distributed; the photons, with intensity I_0, travel through collimator and filter to the patient. Thus, the intensity I_1 can be measured as it is proportional to the photon input energy to the patient. This photon energy interacts with the different layers of matter of the patient, therefore one can measure I_2 at the sensor.
Formulating the physical situation of Fig. 4 in mathematical terms of linear attenuation coef-

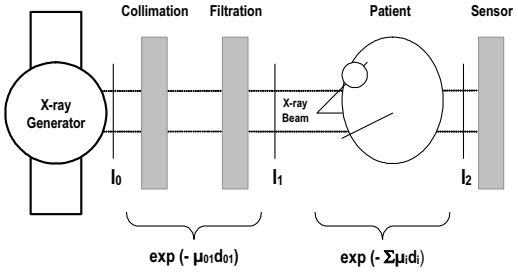

Figure 4: The X-ray Propagation Model.

ficients leads to:

$$I_2 = \underbrace{I_0 \cdot \underbrace{\exp(-\mu_{01}\, d_{01})}_{background\,scatter}}_{I_1} \cdot \underbrace{\exp(-\sum_{i=1}^{K}(\mu_i\, d_i)}_{diagnostic\,scatter} \tag{2}$$

In (2) the intensity I_2 at the sensor is decomposed into the background part I_1, which is further attenuated by the diagnostic part. Photoelectric absorption and Compton scattering, as the main contributors for scattering the beam, induce the contrast function of matter, constisting of K different elements of matter with thickness d_i, which forms the image. Consequently, one may argue, if the fraction $\frac{I_2}{I_1}$ can be calculated, the diagnostic part, namely the distributed mass attenuation factor equivalents can be determined blind[1)], by

$$\ln\left(\frac{I_2}{I_1}\right) = -\sum_{i=1}^{K}(\mu_i\, d_i) \tag{3}$$

The image I_1 can be obtained by an empty scan, taken without a patient, where I_2 is the normal diagnostic image. From (3) the variance of the noise from the diagnostic part is determined by a scatter plot. This noise variance estimate may correct the usually Poisson and Gaussian approach. Unfortunately, in calculating the fraction $\frac{I_2}{I_1}$, one enters the field of Ill-Specified Random Variables [8]. Since I_2 and I_1 can be tract as independent random variables, the dependency of the variance of the quotient of $\frac{I_2}{I_1}$ are

$$\sigma^2 \cong \frac{\sigma_1^2}{m_2^2} + \left(\frac{m_1}{m_2^2}\right)^2 \sigma_2^2 \tag{4}$$

From (4) the original spatial noise contribution σ can be determined, where σ_2^2 is the variance and m_2 the mean of I_2 and σ_1^2 is the variance and m_1 the mean of I_1. Thus, calculating the fraction in the spatial domain leads to a quotient that might be quite poor and the estimated variance may be flawed. Therefore, we have derived a method in the wavelet domain, which enables one to estimate the quotient with aids of the multiresolution support. The method is out of scope of this paper, because of lack of space. It will be published elsewhere.

[1)] It means the separation of a set of independent signals from a set of mixed signals, with at least, only little a priori information about the nature of the signals.

4 The Analysis and Results

The analysis of the nature of given panoramic X-ray images is performed on a large data bank of 2000 samples. A special aluminum phantom was constructed, which supports the ground proof of the analysis. Thus, the collection of several characteristic parameters is maintained. A plot of the standard deviation over the mean of selected samples is given in Figure 5.

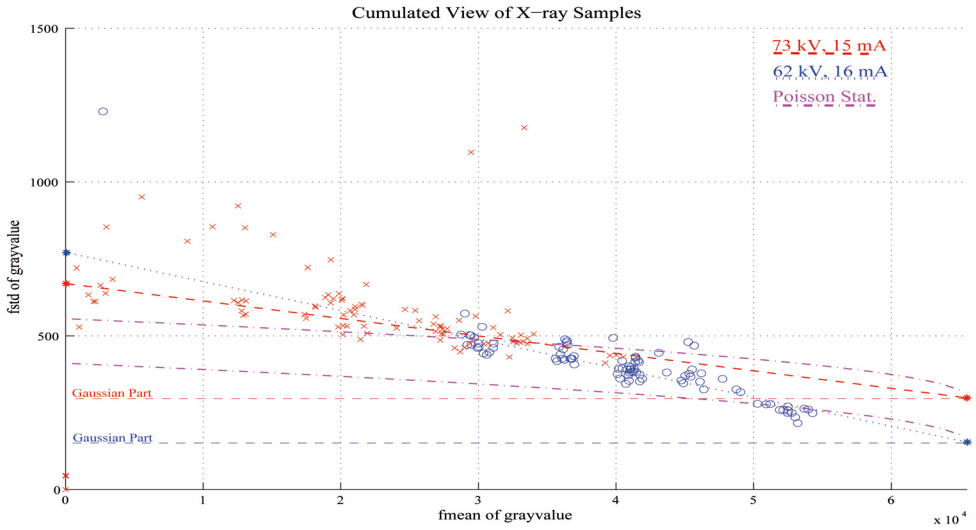

Figure 5: The Statistics Scatter Plot of the Panoramic X-ray images.

Two different operating cases are shown: one at 62 kVp and one at 73 kVp of the X-ray tube. For comparison of both cases, the Poisson equivalent dependences are drawn. The local statistics (mean and variance) are calculated, thus the standard deviation of the real image increases from a changing point on and a gradiental dependency with the kVp value of the two operating cases are in a good match with interaction theory of photons and matter. The increased variance at higher Poisson counts, which are the dark regions of the radiograph, stems from the scattering effects inside the matter. The result confirm the assumptions made on the true noise statistics.

5 Conclusions

In this paper, a new method for estimation of noise is performed by estimation of the diagnostic part of noise, which is derived from an idea of Blind Source Separation [17] to separate the noise from the image's diagnostic and background information. Statistical considerations of X-ray imaging for local density of matter are taken into account. The assessment figures out, that for high photon counts, estimating the noise level by Poisson statistics leads to an underestimated model, whereas for low Poisson counts the variance value is overestimated. This noise variance estimate may correct the usually Poisson and Gaussian approach. Unfortunately, the calculation of the diagnostic part of the noise in the spatial domain leads to

an Ill-specified quotient that might be quite poor and the estimated variance may be flawed. Therefore, we have derived a method in the wavelet domain, which enables one to estimate the quotient with aids of the multiresolution support. The method is out of scope of this paper, because of lack of space. It will be published elsewhere.

References

[1] Aird EGA. Basic Physics for Medical Imaging. *Heinemann, Oxford, 1988*

[2] M. Analoui. Radiographic Image Enhancement. Part I: Spatial Domain Techniques. *Dentomaxillofacial Radiology, Vol 30, Issue 1 1-9, British Institute of Radiology, 2001*

[3] M. Analoui. Radiographic Image Enhancement. Part II: Transform Domain Techniques. *Dentomaxillofacial Radiology, Vol 30, Issue 2 65-77, British Institute of Radiology, 2001*

[4] D.L. Donoho. Denoising by Soft-thresholding. *IEEE Trans. on Information Theory, Vol.41, pp.613-627, 1995*

[5] J. H. Hubbell, S. M. Seltzer Tables of X-Ray Mass Attenuation Coefficients and Mass Energy-Absorption Coefficients (version 1.4). *NISTIR 5632, Nat. Inst. of Stand. and Techn., MD, 1995.*

[6] P. Meer, J. M. Jolion, A. Rosenfeld. A Fast Parallel Algorithm for Blind Estimation of Noise Variance. *IEEE Trans. on Pattern Analysis and Machine Intelligence, Vol.12, No.2, Feb. 1990.*

[7] B. Molander, H-G Gröhndahl and A. Ekestubbe. Quality of film-based and digital panoramic radiography. *Dentomaxillofacial Radiology, Vol 33, 32-36, 2004.*

[8] A. T. Langewisch, F. F. Choobineh. Mean and Variance Bounds and Propagation for Ill-Specified Random Variables. *IEEE Trans. on Systems, Man and Cybernetics, Vol. 34, No.4, July 2004.*

[9] S. I. Olsen. Noise Variance Estimation in Images. *In 8 th Scandinavian Conf. on Image Analysis, Norway, 1993.*

[10] K. Shung, M. Smith, B. Tsui. Principles of Medical Imaging. *Academic Press, 1992.*

[11] Eero P. Simoncelli. Statistical Models for Images: Compression, Restoration and Synthesis. *Asilomar Conf. on Signals Systems, and Computers, Pacific Grove, CA, Nov. 2-5, 1997.*

[12] J. Portilla, Eero P. Simoncelli. Image Restoration using Gaussian Scale Mixtures in the Wavelet Domain. *9th IEEE Int'l Conf on Image Processing. vol. II, pp. 965-968, Barcelona, Spain. September 2003.*

[13] D. J. Simpkin. Radiation Interactions and Internal Dosimetry in Nuclear Medicine. *Radiographics 19:155-167, 1999.*

[14] J.L. Starck, F. Murtagh and A. Bijaoui. Image Processing and Data Analysis: the Multiscale Approach. *Cambridge University Press, 1998.*

[15] J.L. Starck, F. Murtagh Automatic noise estimation from the multiresolution support. *Publ. Astronomic Soc. of the Pacific, 110(744):193-199, 1998.*

[16] JM. Unser, A. Aldroubi and A. Laine. Guest Editorial: Wavelets in Medical Imaging. *IEEE Transactions on Medical Imaging, vol. 22, no. 3, pp. 285-288, March 2003.*

[17] H. Valpola, J. Särela. Accurate, Fast and Stable Denoising Source Separation Algorithms. *Proc. Conf. on ICA and BSS (ICA 2004). Granada, Spain, 22-24 September 2004..*

[18] J. F. Brown and Robert H. Mize On the effect of field structure on differential sensitivity. *Psychological Research (Historical Archive), Springer, vol. 16, no. 1, pp. 355-372, January 1932,*

.